Plasmonics (2018) 13:2369–2376
https://doi.org/10.1007/s11468-018-0763-x

Power-Law/Exponential Transport of Electromagnetic Field in One-Dimensional Metallic Nanoparticle Arrays

Gang Song[1] · **Wei Zhang**[1,2]

Received: 10 March 2018 / Accepted: 25 April 2018 / Published online: 5 May 2018

Abstract

Based on the coupled-dipole analysis and finite-difference time-domain simulation, we have investigated the surface plasmon propagation in one-dimensional metallic nanoparticle (NP) chains. Our systematic studies reveal that the interplay between the localized plasmon excitation and the lattice collective behavior leads to two phases (I and II) of different electromagnetic (EM) field transport properties. In phase I, the EM field decays follow the ***power-law***. In phase II, the EM field shows the ***exponential decay*** in the short-distance regime and the ***power-law decay*** in the long-distance regime. Moreover, universal power-law exponents have been found in the long propagation distance. Different EM field propagation behaviors (power-law decay with different exponents, exponential decay with different propagation length) can be transformed to each other by tuning the parameters of the excitation fields (wavelength, polarization) and/or those of the NP chains. The EM field transport mechanisms we have found are very useful in the design of plasmonic waveguide with both strong field confinement and efficient field/energy transfer, which has important applications in integrated nanophotonic circuits.

Keywords Surface plasmon · Propagations · Power-law decay

Introduction

Extensive studies have been performed on the optical properties and their applications of metallic nanoparticles (NPs), especially the noble metal (such as the gold or the silver) NPs. Metallic NP arrays show interesting collective behaviors (in the absorption/reflection/transmission etc.)[1–6] due to the combination effect of near field and far field, for example, Wood anomaly in the reflection/absorption spectra. Metallic NPs arranged in a line can be used as a waveguide for localized surface plasmon (LSP) propagation [7–28]. The dispersion relationships of the modes for LSP propagating in the chain have been analyzed in both theory and experiment [10–13]. A series of theoretical methods such as the Mie scattering method, and open quantum system approach, were used to describe the characteristics of LSP propagation in metallic NP chains under specific conditions [24–31].

There are a lot of pervious works that point out the exponential decay as the main behavior of the energy transport in metallic nanoparticle chain in most conditions. Some calculation results showed that the non-exponential decay appeared in metallic NP chains [21, 24]. In experiment, the propagation behavior of LSPs with the bright mode showed the non-exponential decay in the chain with close-packed NPs [17]. Though many theoretical and experimental studies have been performed in the past decades, the key factors affecting the LSP propagation in metallic NP arrays are still unclear. It is very important to clarify the propagation behavior of LSP in metallic NP chains, which is very useful in the area of optical communications.

In this paper, taking the silver NP arrays as the sample systems, we apply the coupled-dipole (CD) analysis and the finite-difference time-domain (FDTD) simulation to explore the characteristics of LSP propagating in metallic NP chains. The interplay between the localized plasmon excitation in the individual NP and the lattice collective behavior leads to two phases of different electromagnetic

✉ Wei Zhang
zhang_wei@iapcm.ac.cn

[1] Institute of Applied Physics and Computational Mathematics, P. O. Box 8009(28), Beijing 100088, People's Republic of China

[2] Beijing Computational Science Research Centre, 100084, Beijing, People's Republic of China

(EM) field transport properties. New propagation mechanisms/properties including power-law/exponential decay of EM fields, universal power-law exponents, and modulation methods have been found.

Two Phases of EM Field Propagation

In our system, a series of Ag NPs with the radius R are arranged in a line with the lattice constant l and the incident field polarization angle with respect to the direction of the chain is θ(see the schematic diagram in Fig. 1a). In the coupled-dipole analysis, only the LSP on the first NP is excited by incident light, which could be realized by using a local tip to guide the light onto the first NP in experiment. We first consider the cases of the incident light polarization perpendicular to/parallel to the chain.

The transport of the EM field in one-dimensional (1D) NP chains is mainly determined by the competition between the loss and the interaction among the NPs, which is the combination effect of the individual NP plasmonic property and the collective behavior from the lattice. The plasmonic property of a single NP can be described by the polarizability α_s as [32]:

$$\alpha_s = \frac{3i}{2k^3} \frac{\mu m^2 j_1(m\rho)[\rho j_1(\rho)]' - \mu_1 j_1(\rho)[m\rho j_1(\rho)]'}{\mu m^2 j_1(m\rho)[\rho h_1^1(\rho)]' - \mu_1 h_1^1(\rho)[m\rho j_1(\rho)]'}, \tag{1}$$

where μ and μ_1 are the magnetic permeabilities of the NP and the background, k is the wave-vector in the vacuum, m is the ratio of the index of the metal to that of the background, the dielectric constant of Ag is obtained from the reference [33], j_1 and h_1^1 are the spherical Bessel functions, and $\rho = kR$. This expression is suitable to characterize the optical responses of sphere metal nanoparticles with the radius up to tens of nanometers [32], which also agree with the results calculated by the FDTD method. The collective behavior is due to the coupling between the NPs at different lattice positions. In the cases of $l \gg R$, the interaction between the NP at position nl and the other NP at different lattice position $n'l$ can be described as dipole coupling and can be written as [25]:

$$G_k(r) = \left(\frac{k^2}{|r|} + \frac{ik}{|r|^2} - \frac{1}{|r|^3}\right) e^{ik|r|} \tag{2}$$

with $r = nl - n'l$ for the incident light polarization perpendicular to the chain and

$$G_k(r) = \left(-\frac{2ik}{|r|^2} + \frac{2}{|r|^3}\right) e^{ik|r|} \tag{3}$$

for the incident light polarization along the chain. The coupled-dipole approach works well in the case of $l \geq 3R$ [25–28, 32], which we mainly focus on. Here, we apply it to illustrate the propagation characteristic of the silver NP chains. By solving the coupled-dipole equations for the dipole moments $D_k(nl)$ for NPs at position nl,

$$D_k(nl) = \alpha_s[E_n + \Sigma_{n'} G_k(nl - n'l) D_k(n'l)] \tag{4}$$

with the incident field $E_n = E\delta_{n,0}$, we obtain the dipole moment of each NP in the chain as [25]:

$$D_k(nl) = E \int_{-\pi/l}^{\pi/l} \frac{exp(iqnl)}{1/\alpha_s - S(k,q)} \frac{ldq}{2\pi}, \tag{5}$$

where $S(k,q) = 2\Sigma_{n>0} G_k cos(qnl)$. The analytical structure of $1/\alpha_s - S(k,q)$ has important impact on the propagation characteristics. The systems show quite different EM field transport behaviors depending on whether the resonant condition $Re[1/\alpha_s - S(k,q)] = 0$ can be satisfied. The important role of the analytical structure of $1/\alpha_s - S(k,q)$ reflects the interplay between the individual NP plasmonic properties (α_s) and the collective behavior ($S(k,q)$).

We firstly consider the cases with the incident light polarization perpendicular to the chain ($\theta = 90°$). Here, we use the lattice constant $l = 180$ nm. The chain with NPs of $R = 50$ nm is studied to demonstrate the EM field propagating in Ag NP chains for an incident wavelength $\lambda = 320$ nm as shown in Fig. 1. Here, D_k is normalized as $D_k/E\alpha_s$. The linear relation of $\ln(|I_D|^{1/2})$ [the local field intensity $I_D \propto |D_k|^2$] versus the logarithm of the propagation distance ($\ln(x)$) implies an power-law decay of the EM field for $\lambda = 320$ nm.

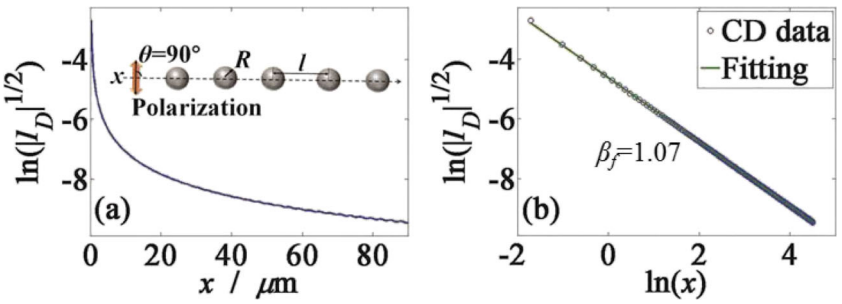

Fig. 1 (Color online) $\ln(|I_D|^{1/2})$ versus the propagation distance x and $\ln(x)$ for $\lambda = 320$ nm, respectively. The incident light polarization is perpendicular to the chain ($\theta = 90°$). Here, CD data is the computation results based on coupled-dipole method

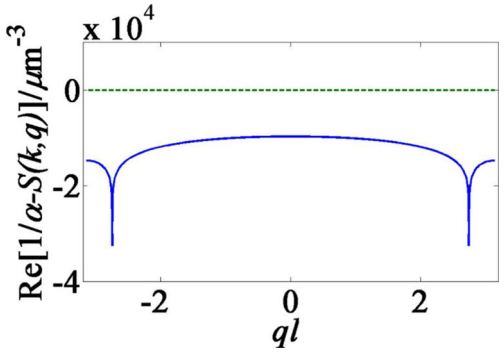

Fig. 2 (Color online) $Re[1/\alpha_s - S(k,q)]$ versus ql for $\lambda = 320$ nm. The incident light polarization is perpendicular to the chain

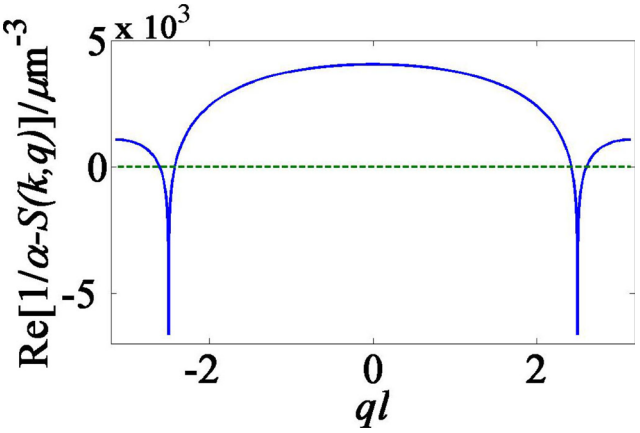

Fig. 4 (Color online) $Re[1/\alpha_s - S(k,q)]$ versus ql for $\lambda = 440$ nm. The incident light polarization is perpendicular to the chain

At this wavelength, $Re[1/\alpha_s - S(k,q)]$ is always nonzero as shown in Fig. 2, then the field decay is according to a power-law. At the wavelength $\lambda = 320$ nm, the absolute value of $1/\alpha_s$ is larger than that of $S(k,q)$. From Eq. 5, we can use perturbation theory and obtain $D_k = \alpha_s^2 S_k E = (\alpha_s E) S_k \alpha_s$, where $S_k(nl) = \int e^{iqnl} S(k,q) l dq/2\pi$. Here, we have the physical picture: $(\alpha_s E)$ describes the dipole moment of a NP with polarizability (α_s), S_k describes the propagation of the dipole field, and the second α_s describes the coupling with the other NP. D_k or S_k shows a universal power-law decay behavior, i.e., $D_k \sim 1/x^\beta$, $\beta = 1$ in the long propagation distance limit. The universal power-law exponent is independent of the material, the size of the nanoparticle. We fit the data from Fig. 1b and obtain the slope -1.07. The difference between the fitting power-law exponent $\beta_f = 1.07$ and $\beta = 1$ is due to the finite fitting propagation distance.

The EM field propagation is determined by the analytical structure of $1/\alpha_s - S(k,q)$ (as seen from Eq. 5), which depends on the wavelength. Then, we take another wavelength to show the other phase of the EM field propagation. $\lambda = 440$ nm is adopted as the working wavelength. $\ln(|I_D|^{1/2})$ versus the propagation distance x and $\ln(x)$ are shown in Fig. 3, respectively. At $\lambda = 440$ nm, the linear relation of $\ln(|I_D|^{1/2})$ versus x indicates the exponential decay in the regime of x from the beginning to about 4 μm as shown in the insert of Fig. 3a, while the linear relation of $\ln(|I_D|^{1/2})$ versus $\ln(x)$ implies the power-law decay in the regime of $\ln(x)$ from 1.81 ($x \sim 6.12$ μm) to the end. Thus, the EM field propagates following an ***exponential law*** in the short-distance regime and a ***power-law*** in the long-distance regime (***exponential decay*** + ***power-law decay***).

The curve of $Re[1/\alpha_s - S(k,q)]$ versus ql for $\lambda = 440$ nm is shown in Fig. 4. One can see that there are solutions q_j ($j = 1, 2...$) to the equation $Re[1/\alpha_s - S(k,q)] = 0$. As seen from Fig. 4, the solution q_j is around $\pm k$. It is related to the singularity around $q \pm k$, which is caused by the long-range coulomb interaction and has the same origin as the Wood anomaly. For simplicity, we consider a solution $\bar{q}$. The generalization to the case with multiple solutions is straightforward. Near $\bar{q}$, $1/\alpha_s - S(k,q) \simeq \frac{\partial ReS(k,q)}{\partial q}|_{q=\bar{q}}(q-\bar{q}) + i\eta \equiv Y$, $\eta = Im(1/\alpha_s - S(k,\bar{q}))$. Then, we can rewrite Eq. 5 into two parts as:

$$D_k(nl) = E\int_{-\pi/l}^{\pi/l} \frac{e^{iqnl}}{Z}\frac{ldq}{2\pi} = E\int_{-\pi/l}^{\pi/l} \frac{e^{iqnl}}{Y}\frac{ldq}{2\pi} + E\int_{-\pi/l}^{\pi/l} \frac{e^{iqnl}}{X}\frac{ldq}{2\pi}, \quad (6)$$

where $Z = 1/\alpha_s - S(k,q)$, $1/X = 1/Z - 1/Y$. The first term on the right hand of Eq. 6 is in the form of $e^{-nl/L}$ ($L = \frac{1}{\eta}|\frac{\partial S(k,q)}{\partial q}|_{q=\bar{q}}$), showing an exponential decay behavior.

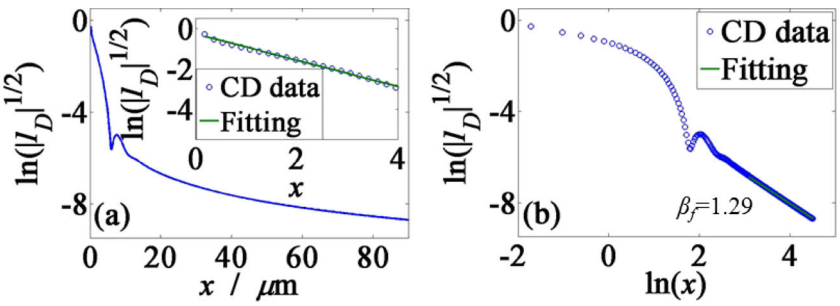

Fig. 3 (Color online) $\ln(|I_D|^{1/2})$ versus the propagation distance x and $\ln(x)$ for $\lambda = 440$ nm, respectively. The incident light polarization is perpendicular to the chain

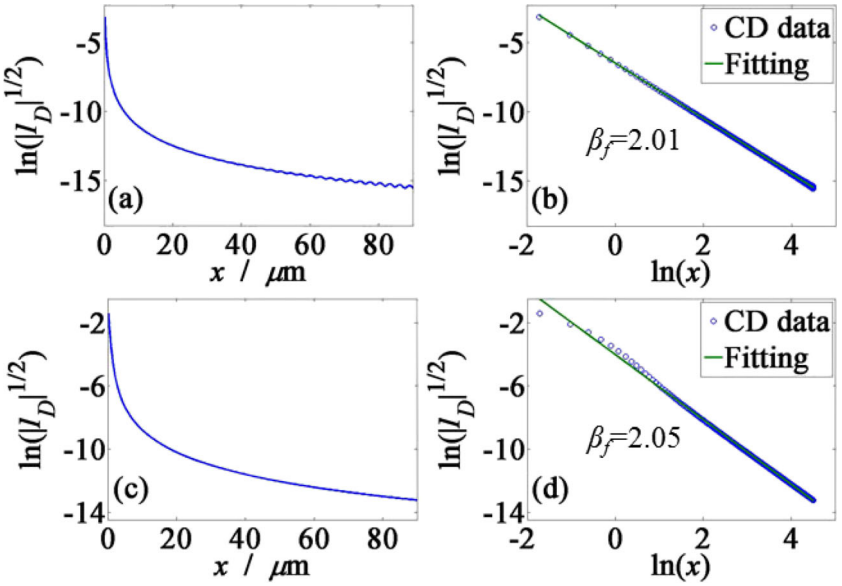

Fig. 5 (Color online) $\ln(|I_D|^{1/2})$ versus the propagation distance x and $\ln(x)$ for $\lambda = 320$ nm (**a**–**b**) and 440 nm (**c**–**d**), respectively. The incident light polarization is parallel to the chain

While for the second term, $Re(X) \simeq \frac{2(\partial S/\partial q)^2}{\partial^2 S/\partial q^2}|_{q=\bar{q}}$ at $q = \bar{q}$. Considering the very fast change of Z with q near $\bar{q}$ and the regularization of the singularity of $1/Z$ ($1/Z \to 1/X = 1/Z - 1/Y$), the second term shows power-law decay as that in Fig. 1. We can obtain the power-law exponent as 1.29 from fitting the data in Fig. 3b and the propagation length as 1.54 μm from fitting the data in Fig. 3a. We note that the propagation length is 500 nm for the lowest mode of Ag nanowire of radius 500 nm. One can see clearly that the inter-particle interaction leads to profound collective effect. It not only affects the propagation length (partially by adding correction to the imaginary part of $1/\alpha_s$, see Eq. 6, but also brings power-law decay in the long-distance regime.

Then, the polarization of incident light along the chain ($\theta = 0°$) is considered. By observing Eqs. 2 and 3, we can see that the Wood anomaly-like singularity disappears and expect some changes in the propagation/transport behavior. The curves of $\ln(|I_D|^{1/2})$ versus the propagation distance x and $\ln(x)$ for $R = 50$ nm, $l = 180$ nm, $\lambda = 320$ nm, and 440 nm are shown in Fig. 5, respectively. The clear linear relation of $\ln(|I_D|^{1/2})$ versus $\ln(x)$ indicates a power-law decay of the EM fields.

As shown in Fig. 6, there is no solution to the equation $Re[1/\alpha_s - S(k,q)] = 0$ for these two wavelengths $\lambda = 320$ and 440 nm. It is quite different from the case with the polarization perpendicular to the chain (Figs. 2 and 4), which is related to the disappearance of Wood anomaly-like singularity. Moreover, the power index should also be different. From Eq. 3, the universal power-law exponent should be 2 in this case. We fit the data from Fig. 5b, d and obtain the slope -2.01 and -2.05 in the long propagation distance regime, respectively. There may also exist a small intermediate wavelength range in which there are some q_0 to make $Re[1/\alpha_s - S(k,q)] = 0$. And the propagation behavior is the exponential decay + power-law decay.

Here, we would like to note that when there is zero of $Re[1/\alpha_s - S(k,q)]$, the system shows a combination of exponential decay and power-law decay. In the long-distance regime, the power-law decay dominates. In the short-distance regime, it is also possible that the contribution of the power-law decay term is larger than that

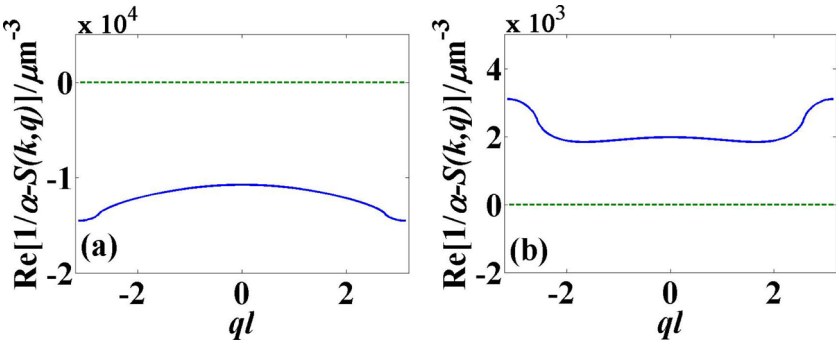

Fig. 6 (Color online) $Re[1/\alpha_s - S(k,q)]$ versus ql for $\lambda = 320$ nm (**a**) and 440 nm (**b**), respectively. The incident light polarization is parallel to the chain

of the exponential decay term. Then the system shows the effective power-law decay behavior, for example for the case with $\lambda = 900$ nm.

To further support our study based on coupled-dipole analysis, we perform the FDTD simulation of the EM field propagation. In the simulation, the chain has 200 silver nanoparticles with radius of 50 nm and the lattice constant is 180 nm. A dipole source is located at a distance of $l = 180$ nm to the first nanoparticle along the chain. The polarization of the dipole source is perpendicular/parallel to the chain. The detecting point is on the side of the nanoparticle with 2.5 nm away from the interface of the nanoparticle along the direction of the dipole. The incident field wavelengths are 320 and 440 nm. The gird is 2.5 nm. The detecting EM field intensity is I_D. $\ln(|I_D|^{1/2})$ versus $\ln(x)$ (x the propagation distance) is shown in Fig. 7.

From Fig. 7a, b, we find two different field transport characteristics for the source dipole perpendicular to the chain. The linear relation of $\ln(|I_D|^{1/2})$ versus $\ln(x)$ in Fig. 7a indicates a power-law decay of EM field with the slope of –1.08 for $\lambda = 320$ nm. Figure 3 shows an exponential decay + power-law decay of the EM field for $\lambda = 440$ nm based on CD method. Here, as shown in Fig. 7b, the linear relation of $\ln(|I_D|^{1/2})$ versus $\ln(x)$ is in the regime from about $1.81 (x \sim 6.12\ \mu$m) to the end, which implies an ***exponential decay + power-law decay*** of EM field with the slope of -1.35 for $\lambda = 440$ nm. The derivation of the exponent from 1 is due to the finite fitting regime. From Fig. 7c, d, the linear relations of $\ln(|I_D|^{1/2})$ versus $\ln(x)$ for the the polarization of the source dipole along the chain indicate the power-law decay of EM field with the slopes of -1.99 and -2.09, respectively. The power-law exponents based on the coupled-dipole calculations and the FDTD simulations are listed in Table 1.

Table 1 The power-law exponents from the coupled-dipole (CD) calculations and FDTD simulations

	CD	FDTD
$\lambda = 320$ nm, $\perp$	-1.07	-1.08
$\lambda = 440$ nm, $\perp$	-1.29	-1.35
$\lambda = 320$ nm, $\parallel$	-2.01	-1.99
$\lambda = 440$ nm, $\parallel$	-2.05	-2.09

As shown in Table 1, EM field transport characteristics and the power-law exponents from the FDTD simulations agree well with those based on coupled-dipole analysis.

Universality and Modulation of EM Field Propagation

We have shown that there are two phases of the EM field propagation in 1D metallic NP chains, which are determined by the analytical structure of $1/\alpha_s - S(k, q)$. The parameters of the excitation field and the structure of the NP chains have important impacts on the EM field transport behavior. As discussed above, the two phases of the EM field propagation can be transformed to each other by tuning the wavelength of the excitation field.

We further explore the EM field propagation with excitation fields of different polarizations. The calculation results in Fig. 8 show that the EM field propagates according to power-law for $\lambda = 320$ nm. The power-law exponents is 1.08 for incident field polarization angles 30°, 45°, 60°, and 90° with respect to the direction of the chain. The power-law exponents is 1.99 for the polarization angle 0°.

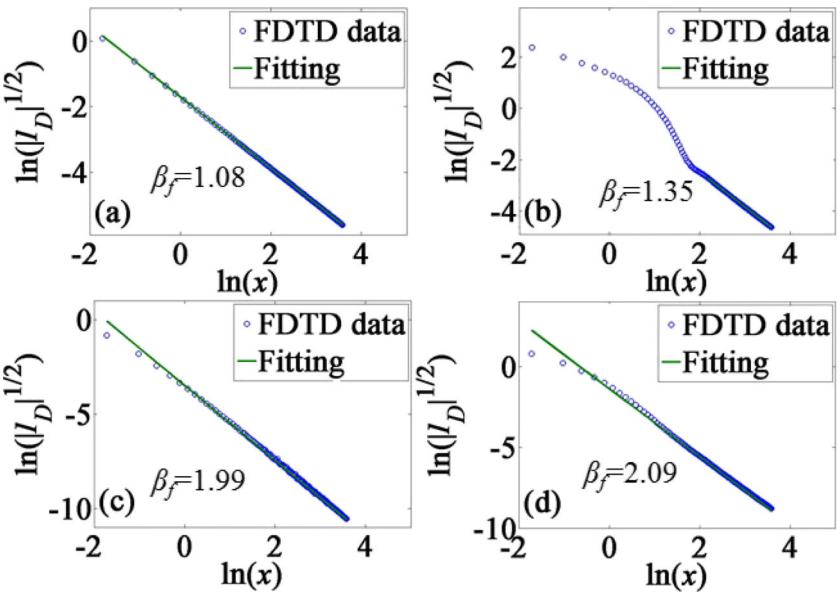

Fig. 7 (Color online) $\ln(|I_D|^{1/2})$ versus $\ln(x)$ for the polarization of the source dipole perpendicular to (**a**, **b**) /parallel to (**c**, **d**) the chain with $\lambda = 320$ nm (**a**, **c**) and 440 nm (**b**, **d**), respectively. I_D is the EM field intensity, and x is the propagation distance

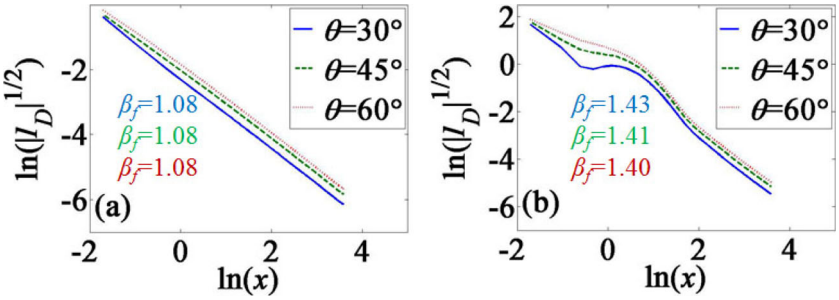

Fig. 8 ((Color online) $\ln(|I_D|^{1/2})$ versus $\ln(x)$ for the polarization angles 0°, 30°, 45°, 60°, 90° of the source dipole with respect to the direction of the Ag chain. **a** $\lambda = 320$ nm and **b** $\lambda = 440$ nm

In the presence of excitation fields with wavelength $\lambda = 440$ nm and polarization angles 30°, 45°, 60°, and 90°, the EM field propagates following exponential law in the short-distance regime and power-law in the long-distance regime. The power-law exponents are 1.43, 1.41, 1.40, and 1.35 for polarization angles 30°, 45°, 60°, and 90°. These power-law exponents obtained by fitting the $\ln(|I_D|^{1/2}) - \ln(x)$ curves in the regimes of finite propagation distance show the combination power-law decay of EM field with exponents 1 and 2. In the very long propagation distance regime, the leading contribution is the power-law decay with exponent 1. For the case of incident field polarization angle 0°, the EM field propagates following the power-law with exponent 2.09 (by fitting the calculation data in finite propagation distance). Therefore, by tuning the incident field (wavelength and polarization), one can achieve different EM field transport behaviors, i.e., power decay (with different exponents) and exponential decay (with different propagation length)+power-law decay. This modulation of light transport through controlling polarization has practical applications. For example, one may change the polarization state α of the light before transport into another state β by wave plate. Then after the transportation of light with polarization state β, the polarization state β can be changed back into state α. In this way, the EM field transport property of polarization state β has been utilized.

The geometric parameters of the NP chain also play an important role in the EM field transport. The calculation results of EM field propagation in metallic chains with Ag NPs of radius $R = 40$, 45 , and 55 nm are shown in Fig. 9. The general power-law decay of EM field has been found for the cases with the wavelength $\lambda = 320$ nm (incident field polarization parallel to/ perpendicular to the chain) and the wavelength $\lambda = 440$ nm (the incident field polarization parallel to the chain) as shown in Fig. 9a, b, c. While for $\lambda = 440$ nm (incident field polarization perpendicular to the chain), the EM field transport behavior is exponential decay + power-law decay with the intensity propagation lengths of 43 , 3.88 , and 0.56 μmm, respectively. For NPs with different sizes, the contributions from the exponential decay and the power-law decay are different, which leads to the

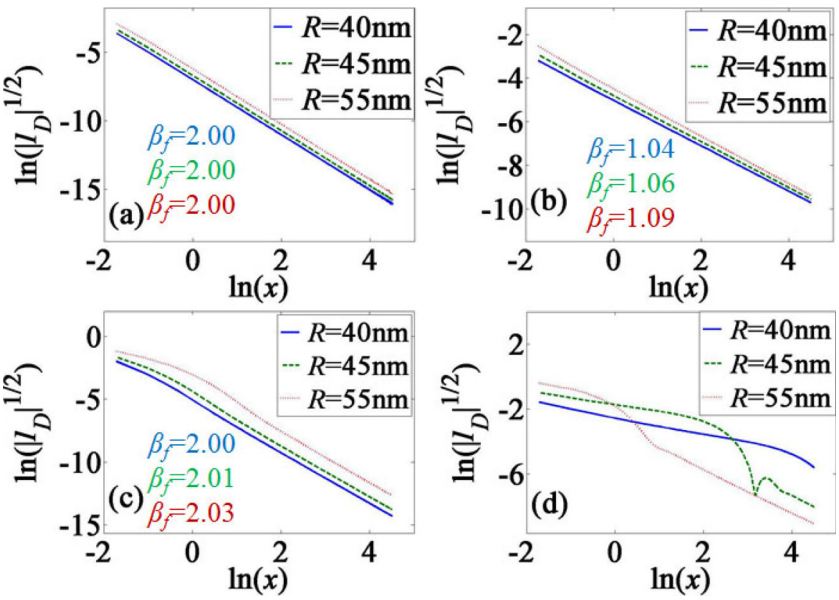

Fig. 9 (Color online) $\ln(|I_D|^{1/2})$ versus $\ln(x)$ for Ag chains with particles of radius $R = 40$, 45 , 55 nm, respectively. The polarization of the source dipole is parallel to (**a**, **c**) /perpendicular to (**b**, **d**) the chain with $\lambda = 320$ nm (**a**, **b**) and 440 nm (**c**, **d**), respectively

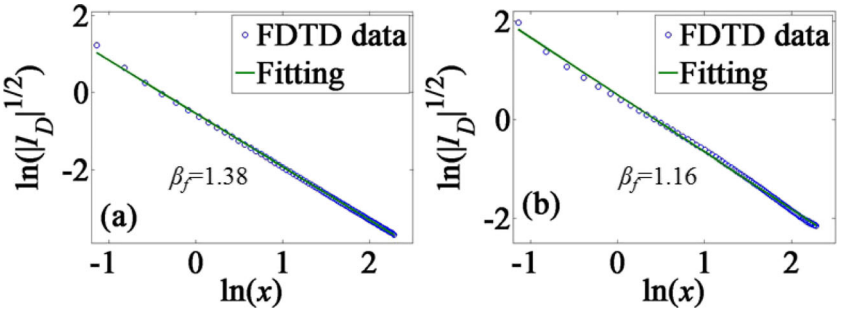

Fig. 10 (Color online) $\ln(|I_D|^{1/2})$ versus $\ln(x)$ for the polarization of the source dipole perpendicular to Ag chain for $\lambda = 300$ nm (**a**) and Au chain for $\lambda = 514$ nm (**b**), respectively. I_D is the EM field intensity, and x is the propagation distance

change of the transition point (from the exponential decay to the power-law decay).

We have focused our studies on the systems with large lattice constant ($l > 3R$), in which the CD method works well as supported by the FDTD simulations. By using CD method, we are able to provide analytical solutions and clear physical picture/mechanism, also gives the universal power-law exponents. We then consider the cases of lattice constant smaller than $3R$. We use FDTD method to study the propagation behavior of NP chains with $l < 3R$. In the calculation, we use the NP chain with $R = 50$ nm, $l = 120$ nm. Silver and Gold NPs are all considered to demonstrate the universality of the propagation property. The dielectric constants are obtained from the reference [33]. The incident field polarization is perpendicular to the chain and the wavelength λ is 300 nm for Ag NP chain and 514 nm for Au NP chain. $\ln(|I_D|^{1/2})$ versus $\ln(x)$ are shown in Fig. 10. As shown in Fig. 10, both the two lines show the linear relation with $\ln(x)$. We fit the two lines and the two slopes are -1.38 and -1.16. These results point that the power-law decay may also appear in different metallic NP chains with different lattice constants.

The non-exponential decay was also pointed out in the experiment with close-packed NP chain [17]. The experiment data can be replotted in the double logarithm form as shown in Fig. 11. The linear relation between $\ln(|I_D|^{1/2})$ versus $\ln(x)$ (x the propagation distance) indicate a power-law decay of EM field. The pow-law exponent is 1.38. Hence, our analytical and simulation methods provide new ways to clarify the propagation behaviors in 1D metallic NP chains in previous studies [17, 21, 24].

Conclusions

In summary, we have studied the characteristics of the LSP propagation in one-dimensional metallic nanoparticle chain based on the coupled-dipole calculations and FDTD simulations. The LSP propagation shows different behaviors in different phases, depending on the analytical structure of $1/\alpha_s - S(k, q) = 0$, which is determined by both the individual NP plasmonic property and the lattice collective effect. In phase I, a power-law decay of EM field has been identified. While in phase II, EM field propagates in the form of the exponential decay+power-law decay, i.e., exponential decay in the short-distance regime and power-law decay in the long-distance regime. The universal power-law exponents have been found for EM field propagation in the long propagation distance regime. The results of FDTD simulations agree well with our theoretical predictions based on coupled-dipole method. It is found that by tuning the incident field (wavelength and polarization) and the geometric parameters of the NP chains, one can achieve different EM field transport behaviors, i.e., power decay (with different exponents) and exponential decay+power-law decay. Our studies reveal a general picture of the EM field transport in nanoparticle chains, which have applications in the plasmonic waveguide and integrated nanophotonic circuits.

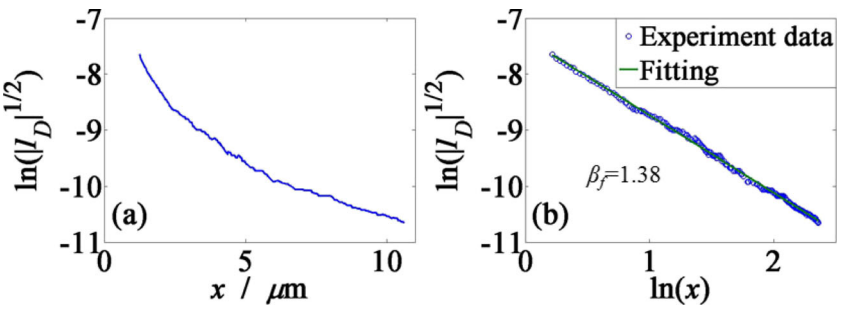

Fig. 11 (Color online) **a** $\ln(|I_D|^{1/2})$ versus the propogation distance x based on the the experiment data at $\lambda = 514$ nm [17]; **b** $\ln(|I_D|^{1/2})$ versus $\ln(x)$ for $\lambda = 514$ nm

Funding Information This work was partially supported by National Key Research and Development Program of China (Grant No. 2017YFA0303400), National Natural Science Foundation of China (Grant Nos. 11774036, 11374039).

References

1. Wood RW (1902) On a remarkable case of uneven distribution of light in a diffraction grating spectrum. Proc Phys Soc Lond 18:269–275
2. Auguié B, Barnes WL (2008) Collective resonances in gold nanoparticle arrays. Phys Rev Lett 101:143902
3. Haes AJ, Van Duyne RP (2004) A unified view of propagating and localized surface plasmon resonance biosensors. Anal Bioanal Chem 379:920–930
4. Fischer MP, Schmidt C, Sakat E, Stock J, Samarelli A, Frigerio J, Ortolani M, Paul DJ, Isella G, Leitenstorfer A, Biagioni P, Brida D (2016) Optical activation of germanium plasmonic antennas in the mid-infrared. Phys Rev Lett 117:047401
5. Ma J, Pesin DA (2017) Dynamic chiral magnetic effect and Faraday rotation in macroscopically disordered helical metals. Phys Rev Lett 118:107401
6. Ling CW, Xiao M, Chan CT, Yu SF, Fung KH (2015) Topological edge plasmon modes between diatomic chains of plasmonic nanoparticles. Opt Express 23:2021
7. Song G, Wei Zhang (2017) Electromagnetic field propagation in the one-dimensional silver nanoparticle dimer chains: hotspots and energy transport. Plasmonics 12:179–184
8. Maier SA, Kik PG, Atwater HA, Meltzer S, Harel E, Koel BE, Requicha AAG (2003) Local detection of electromagnetic energy transport below the diffraction limit in metal nanoparticle plasmon waveguides. Nat Mater 2:229–232
9. Maier SA, Kik PG, Atwater HA (2002) Observation of coupled plasmon-polariton modes in Au nanoparticle chain waveguides of different lengths: estimation of waveguide loss. Appl Phys Lett 81:1714–1716
10. Pike NA, Stroud D (2013) Plasmonic waves on a chain of metallic nanoparticles: effects of a liquid-crystalline host. J Opt Soc Am B 30:1127–1134
11. Park SY, Stroud D (2004) Surface-plasmon dispersion relations in chains of metallic nanoparticles: an exact quasistatic calculation. Phys Rev B 69:125418
12. Crozier KB, Togan E, Simsek E, Yang T (2007) Experimental measurement of the dispersion relations of the surface plasmon modes of metal nanoparticle chains. Opt Express 15:17482–17493
13. Yang T, Crozier KB (2008) Dispersion and extinction of surface plasmons in an array of gold nanoparticle chains: influence of the air/glass interface. Opt Express 16:8570–8580
14. Kravets VV, Ocola LE, Khalavka Y, Pinchuk AO (2015) Polarization and distance dependent coupling in linear chains of gold nanoparticles. Appl Phys Lett 106:053104
15. Stepanov AL, Krenn JR, Ditlbacher H, Hohenau A, Drezet A, Steinberger B, Leitner A, Aussenegg FR (2005) Quantitative analysis of surface plasmon interaction with silver nanoparticles. Opt Lett 30:1524–1526
16. Xiao JJ, Yakubo K, Yu KW (2006) Dispersion and transitions of dipolar plasmon modes in graded plasmonic waveguides. Appl Phys Lett 89:221503
17. SolisJr D, Willingham B, Nauert SL, Slaughter LS, Olson J, Swanglap P, Paul A, Chang WS, Link S (2012) Electromagnetic energy transport in nanoparticle chains via dark plasmon modes. Nano Lett 12:1349–1353
18. SolisJr D, Paul A, Olson J, Slaughter LS, Swanglap P, Chang WS, Link S (2013) Turning the corner: efficient energy transfer in bent plasmonic nanoparticle chain waveguides. Nano Lett 13:4779–4784
19. Yin LL, Vlasko-Vlasov VK, Pearson J, Hiller JM, Hua J, Welp U, Brown DE, Kimball CW (2005) Subwavelength focusing and guiding of surface plasmons. Nano Lett 5:1399–1402
20. Radko IP, Bozhevolnyi SI, Evlyukhin AB (2007) A surface plasmon polariton beam focusing with parabolic nanoparticle chains. Opt Express 15:6576–6582
21. Willingham B, Link S (2011) Energy transport in metal nanoparticle chains via sub-radiant plasmon modes. Opt Express 19:6450–6461
22. Barrow SJ, Funston AM, Gomez DE, Davis TJ, Mulvaney P (2011) Surface plasmon resonances in strongly coupled gold nanosphere chains from monomer to hexamer. Nano Lett 11:4180–4187
23. Fevrier M, Gogol P, Aassime A, Megy R, Delacour C, Chelnokov A, Apuzzo A, Blaize S, Lourtioz JM, Dagens B (2012) Giant coupling effect between metal nanoparticle chain and optical waveguide. Nano Lett 12:1032–1037
24. Quinten M, Leitner A, Krenn JR, Aussenegg FR (1998) Electromagnetic energy transport via linear chains of silver nanoparticles. Opt Lett 23:1331–1333
25. Markel VA, Sarychev AK (2007) Propagation of surface plasmons in ordered and disordered chains of metal nanospheres. Phys Rev B 75:085426
26. Rasskazov IL, Karpov SV, Markel VA (2013) Nondecaying surface plasmon polaritons in linear chains of silver nanospheroids. Opt Lett 38:4743–4746
27. Rasskazov IL, Karpov SV, Markel VA (2014) Waveguiding properties of short linear chains of nonspherical metal nanoparticles. J Opt Soc Am B 31:2981–2989
28. Rasskazov IL, Karpov SV, Markel VA (2014) Surface plasmon polaritons in curved chains of metal nanoparticles. Phys Rev B 90:075405
29. Brandstetter-Kunc A, Weick G, Downing CA, Weinmann D, Jalabert RA (2016) Nonradiative limitations to plasmon propagation in chains of metallic nanoparticles. Phys Rev B 94:205432
30. Downing CA, Mariani E, Weick G (2017) Retardation effects on the dispersion and propagation of plasmons in metallic nanoparticle chains. J Phys.: Condens Matter 30:025301
31. Fung KH, Tang RCH, Chan CT (2011) Analytical properties of the plasmon decay profile in a periodic metal-nanoparticle chain. Opt Lett 36:2206
32. Zou SL, Schatz GC (2006) Theoretical studies of plasmon resonances in one-dimensional nanoparticle chains: narrow lineshapes with tunable widths. Nanotechnology 17:2813–2820
33. Lynch DW, Hunter WR (1985) Silver (Ag). In: Palik ED (ed) Handbook of optical constants of solids. Academic, New York